# Supporting Information

**Exsolution of Catalytically Active Iridium Nanoparticles from Strontium Titanate**

Eleonora Calì[†]*, Gwilherm Kerherve[†], Faris Naufal[†], Kalliopi Kousi[‡], Dragos Neagu[¶], Evangelos I. Papaioannou[‡], Melonie P. Thomas[§], Beth S. Guiton[§], Ian S. Metcalfe[‡], John T. S. Irvine[||], David J. Payne[†]*

[†]Department of Materials, Imperial College London, Exhibition Road, London SW7 2AZ, United Kingdom
E-mail: e.cali14@imperial.ac.uk; d.payne@imperial.ac.uk
[‡]School of Engineering, Newcastle University, Merz Court, Newcastle upon Tyne NE1 7RU, United Kingdom
[¶]Chemical & Process Engineering, University of Strathclyde, Glasgow, G1 1XL, United Kingdom
[§]Department of Chemistry, University of Kentucky, 505 Rose Street, Lexington, Kentucky 40506, USA
[||]School of Chemistry, University of St Andrews, St Andrews, KY16 9ST, United Kingdom

## S1. Image Analysis and Calculations

Particle size distribution and particle density were analyzed using ImageJ software. In order to calculate the number of exsolved Ir atoms ($N_{Ir_{exsolved}}$), the particles size and surface distribution (NP µm$^{-2}$) were integrated in the following calculations, based on similar work described previously: [1,2]

$$N_{Ir_{exsolved}} = \frac{4\pi\rho_{Ir}N_A}{3A_{Ir}}\sum_i f_i(\frac{d_i}{2})^3$$

Where $\rho_{Ir}$ is density of Ir, $N_A$ is the Avogadro's number, $A_{Ir}$ is the atomic weight of Ir, $f_i$ the fraction of exsolved nanoparticles (per µm$^{-2}$ of perovskite) with diameter $d_i$.

The average number of Ir atoms in a perovskite grain of length $L$, width $W$ and depth $d$ was then calculated assuming a parallelepiped grain shape:

$$N_{Ir_{grain}} = \frac{LWd}{a_p^3}x_{Ir}$$

where $x_{Ir}$ is the nominal doping concentration (x=0.5%).

By calculating the average surface area of one grain, it is possible to convert $N_{Ir_{exsolved}}$ in the number of exsolved Ir atoms per grain, which allowed us to calculate the concentration % of Ir exsolved compared to our nominal doping concentration (exsolved Ir concentration %= ∼0.2).

The total number of exsolved Ir atoms analysed in the XPS spot probing area ($N_{Ir_{XPS}}$) was then calculated, and related to the total number of Ti atoms analysed in the probing volume of XPS spot ($N_{Ti_{XPS}}$), considering a probing depth of 10 nm:

$$N_{Ti_{XPS}} = \frac{400 \times 0.01}{a_p^3}x_{Ti}$$

By relating this number to the Ti nominal concentration and comparing it with $N_{Ir_{XPS}}$, it was then possible to calculate the expected Ir concentration (%) in the probing XPS spot volume, which, for the sample reduced at the highest temperature, was calculated as ∼2%, in good agreement with the 1.6% measured by XPS.

## S2. Supplementary Data

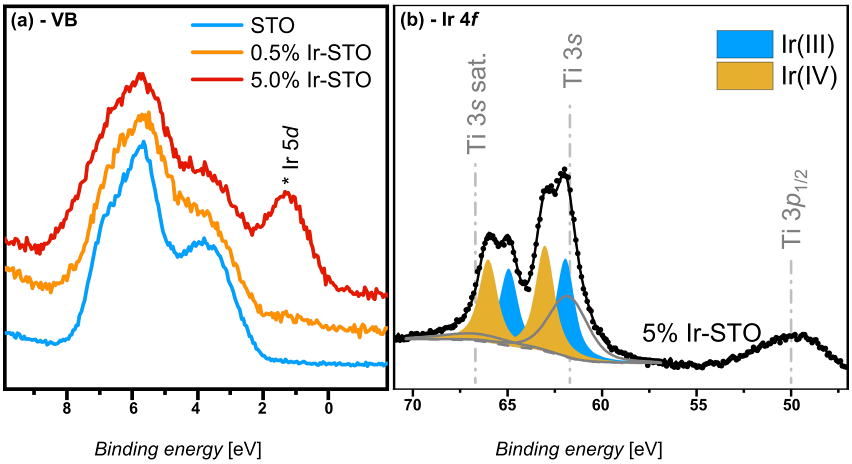


Figure S1: XPS analysis showing a) the valence band comparison for the undoped STO, 0.5% Ir-doped STO, and 5% Ir-doped STO; b) Ir 4*f* core level of 5% Ir-doped STO showing both $Ir^{4+}$ and $Ir^{3+}$ components.

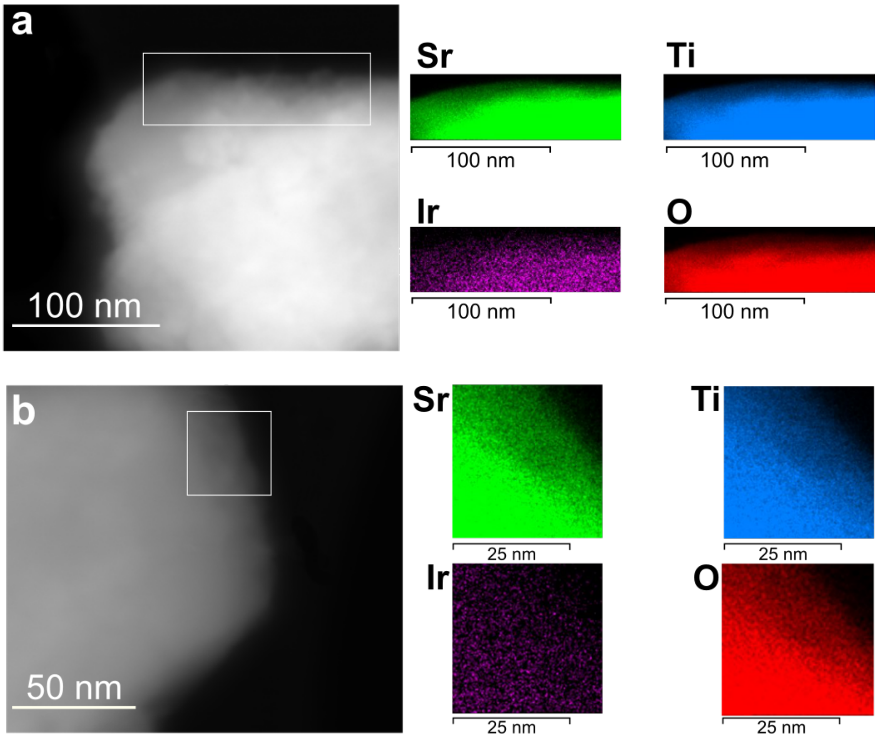


Figure S2: STEM-EDX elemental analysis carried out on the as-synthesised 0.5% Ir-doped STO. The areas analysed in the two different Ir-STO grains in a) and b) both show the homogeneous composition of the sample before reduction at high temperatures.

Table S1: XPS fit parameter for the Ir $4f$, Ti $2p$, Sr $3d$ and C $1s$ of the undoped STO, Ir-doped STO and Ir-doped STO reduced at 1100 °C and 1300 °C.

| **Core line** | **BE (eV)** | **FWHM (eV)** | **SOS (eV)** | **Atomic %** |
|---|---|---|---|---|
| **Undoped STO** | | | | |
| Sr $3d_{5/2}$ STO | 132.65 | 0.9 | 1.76 | 39.97 |
| Sr $3d_{5/2}$ $SrCO_3$ | 133.38 | 1.2 | 1.7 | 4.05 |
| Ti $2p_{3/2}$ | 458.13 | 0.99 | 5.75 | 51.82 |
| C $1s$ C=O | 289.25 | 1.51 | — | 4.16 |
| C $1s$ C-C | 284.8 | 1.49 | — | — |
| **Ir doped STO** | $20^{o}$C | | | |
| Ir $4f_{7/2}$ Ir(III) | 61.79 | 1.2 | 3.00 | 0.41 |
| Sr $3d_{5/2}$ STO | 132.52 | 1.09 | 1.76 | 37.61 |
| Sr $3d_{5/2}$ $SrCO_3$ | 133.5 | 1.19 | 1.75 | 12.10 |
| Ti $2p_{3/2}$ | 458.05 | 1.27 | 5.71 | 49.88 |
| C $1s$ C=O | 289.25 | 1.51 | — | 14.76 |
| C $1s$ C-C | 284.8 | 1.45 | — | — |
| **Ir doped STO** | $1100^{o}$C | | | |
| Ir $4f_{7/2}$ Ir(0) | 59.95 | 1.19 | 3.10 | 0.62 |
| Sr $3d_{5/2}$ STO | 132.92 | 1.15 | 1.76 | 36.96 |
| Sr $3d_{5/2}$ $SrCO_3$ | 133.82 | 1.25 | 1.73 | 14.11 |
| Ti $2p_{3/2}$ | 458.4 | 1.29 | 5.78 | 39.96 |
| C $1s$ C=O | 289.66 | 1.41 | — | 8.34 |
| C $1s$ C-C | 284.8 | 1.41 | — | — |
| **Ir doped STO** | $1300^{o}$C | | | |
| Ir $4f_{7/2}$ Ir(0) | 59.80 | 1.00 | 3.07 | 0.65 |
| Sr $3d_{5/2}$ STO | 132.76 | 0.99 | 1.75 | 42.92 |
| Sr $3d_{5/2}$ $SrCO_3$ | 133.74 | 1.09 | 1.7 | 7.76 |
| Ti $2p_{3/2}$ | 458.17 | 1.02 | 5.73 | 39.38 |
| C $1s$ C=O | 289.64 | 1.38 | — | 9.30 |
| C $1s$ C-C | 284.8 | 1.25 | — | — |

Table S2: $Sr_{SrCO_3}$ : $Sr_{lattice}$ before doping, after doping and after exsolution.

| **Samples** | **Sr (surface)** | **Sr (bulk)** |
|---|---|---|
| Undoped STO | 9.2 % | 90.8 % |
| Ir-STO | 24.3 % | 75.7 % |
| Ir-STO, 900 °C | 17.1% | 82.9% |
| Ir-STO, 1100 °C | 27.6 % | 72.4 % |
| Ir-STO, 1300 °C | 15.3 % | 84.7 % |

**References**

[1] C. Tang, K. Kousi, D. Neagu, J. Portolés, E. I. Papaioannou, I. S. Metcalfe, *Nanoscale*, **2019**, 11, 16935.
[2] D. Neagu, T.-S. Oh, D. N. Miller, H. Ménard, S. M. Bukhari, S. R. Gamble, R. J. Gorte, J. M. Vohs, J. T.S. Irvine, *Nature Commun.*, **2015**, 6, 8120.